Results in Physics 65 (2024) 107963

Contents lists available at ScienceDirect

Results in Physics

journal homepage: www.elsevier.com/locate/rinp

Complexity measures of electric screening effect in interstellar medium

Precious O. Amadi [a,c], Suryadi Suryadi [d], Norshamsuri Ali [b,e], Syed Alwee Aljunid [b,e,*], Rosdisham Endut [b,e], Mohd Aminudin Jamlos [b,e], Akpan N. Ikot [f,g]

[a] Institute of Engineering Mathematics, Universiti Malaysia Perlis, 02600, Arau Perlis, Malaysia
[b] Faculty of Electronic Engineering Technology, Universiti Malaysia Perlis, 02600, Arau Perlis, Malaysia
[c] Department of Physics, Ignatius Ajuru University of Education, Rumuolumeni, Port Harcourt, P.M.B 5047, Rivers State, Nigeria
[d] Deparment of Computer Engineering, Bina Nusantara (BINUS) University, Palmerah, West Jakarta, 11480, DKI Jakarta, Indonesia
[e] Centre of Excellence Advanced Communication Engineering (ACE), Universiti Malaysia Perlis (UniMAP), Arau, 02600, Perlis, Malaysia
[f] Theoretical Physics Group, Department of Physics, University of Port Harcourt, PMB 5323, Choba, Rivers State, Nigeria
[g] Western Caspian University, Baku, Azerbaijan

ARTICLE INFO

Keywords:
Shannon entropy
Fisher information
Complexity measures
Interstellar mediums
Probability density
Debye–Huckel length

ABSTRACT

Using the screening potential, we explore probability density properties in interstellar mediums (ISM) in information theory. With the eigenfunctions obtained for the screening potential using the Schrodinger equation, we studied the probability distribution for Shannon entropy, Fisher information, and their complexity measures for the values of n and l. From our numerical result, for Shannon entropy, we observed a more localized probability distribution in position and a decreasing localization in the momentum space as the values of n and l increases. For Fisher information, localization increases in the position space and, consequently, delocalization in their momentum spaces. The uncertainty relations of Shannon entropy and Fisher information were computed and satisfied the relations. For interstellar mediums, our findings align with Heinsberg's uncertainty principle. Complexity measure was also studied for the interstellar mediums and our findings showed increasing disorder in the position space for increasing values of n and l. Furthermore, we extended the Debye-Hückel length to other regimes particularly, Magnetosphere ($D = 10^2$) and Intergalactic Mediums ($D = 10^5$)

Introduction

Plasma systems are characterized by ionized gas that creates an electric field effect due to the presence of mobile charged particles. The forces created cause the charges to act against the electric field within a distance in the order of D, the Debye–Huckel length. The potential energy that describes the Debye screening effect in one dimension is defined as [1],

$$V(x) = \frac{1}{4\pi\varepsilon}\frac{q_1 q_2}{x}e^{-\alpha x} \tag{1}$$

where $\alpha = \left(\frac{1}{D}\right)$, q_1, q_2 are the electrical charges, ε is the permittivity of the system, x is the distance of interacting particles and ranges between zero and infinity, and D is the Debye–Huckel length, also known as the screening length, is a characteristic length scale that describes how charge carriers in a medium (ions and electrons) affects each other's electric fields. It is defined as the distance over which the electric field of a charged particle is screened (or reduced) by the surrounding particles. The screening length is expressed as:

$$D = -2\sqrt{\frac{\beta}{\varepsilon}\sum_{\eta=1}^{\eta=N} n_\eta^0 q_\eta^2} \tag{2}$$

where, $\beta = (K_b T)^{-1}$, T is the absolute temperature, K_b the Boltzmann constant, N is the total number of species in the system, and n_η^0 is the mean volumetric density of the charge of the species. The screening length or Debye–Huckel length is the distance at which the magnitude of the electrostatic field is reduced to $\frac{1}{e}$ from its original value. The applications of screening potential in physics are in the area of plasma [2], semiconductors [3], radioactive transition [4], etc. The screening length determines the range over which electrostatic interactions between charged particles are attenuated. A smaller screening length indicates stronger electrostatic interactions and longer-range influence, while a larger screening length indicates weaker interactions and shorter-range influence.

* Corresponding author.
E-mail addresses: amadiwati@gmail.com (P.O. Amadi), suryadi008@binus.ac.id (S. Suryadi), norshamsuri@unimap.edu.my (N. Ali), syedalwee@unimap.edu.my (S.A. Aljunid), rosdisham@unimap.edu.my (R. Endut), mohdaminudin@unimap.edu.my (M.A. Jamlos).

https://doi.org/10.1016/j.rinp.2024.107963
Received 1 September 2023; Received in revised form 30 August 2024; Accepted 6 September 2024
Available online 14 September 2024

The attention that has been drawn to the plasma environment is because of the presence of the attractive field. The Debye screening is vital in this area as it plays a crucial role in the study of the plasma environment. Also, the screening element is the potential factor that determines the interatomic forces. Researchers have carried out studies on the influence of screening effect on plasma systems. Soyl investigated how much influence the screening effect has on the energy of the hydrogen atom [5] and astrophysical nuclear reactions [6] using the more general exponential cosine screened potential (MGECSP). The screened Coulomb has been used to study the screening effect on hydrogen atoms in weakly coupled plasma [7], for different Debye lengths [8], and in information theory [9]. External electric field screening effect has also been introduced on hydrogen atoms [10]. The screening parameter term of the potential, when varied, can influence the increase or decrease of energy values on the hydrogen atom.

The focus of our study is interstellar mediums. Matter and radiation occupy the region of space between interstellar systems. The primary component of the interstellar mediums is hydrogen, and a fraction of the other components of dusty particles are held together by gravitational force and also exhibit variation in temperature, density, and ionization properties [11]. This variation is caused by the surrounding plasma, which affects the distribution of the system. One of the properties of concern that motivated the study is density (or electron density) distribution in interstellar mediums. Understanding the interstellar mediums' physical properties, particularly the probability density distribution, is crucial for predicting particle behaviour and localization within this medium. This study extends the concept of electrical screening potential, typically described by the Debye–Hückel length, to investigate its information entropy, including Shannon entropy [12], Fisher information [13], and their complexity measures [14]. Several research contributions have been made in information entropies including, Abdel-Hady and Nasser [15] used the Modified Hulten potential to study Fisher–Shannon product, and Nagy [16] also studied a two-electron entangled artificial atom in this domain. Some potentials that have been studied include, Morse Oscillator [17], Eckart [18], confined Hydrogen atom [19] Deng-Fan Eckart [20], screened Kratzer [21], Generalized hyperbolic [22], and many more [23–30].

In this work, we investigate the electrical screening effect and how it affects the probability density for interstellar mediums leveraging quantum information entropy. We analyse density property in the position and momentum space for various quantum numbers n from $n = 1$ to $n = 4$ in one dimension for Shannon entropy, Fisher information, and their complexity measures as shown in the flow chart in Fig. 1.

Our result is a complementary behaviour of localization and delocalization characteristics which aligns with the uncertainty principle. The rest of the paper is presented as follows. In Section "Eigen solution", we will obtain energy and wavefunctions for the electrical screening potential using the NUFA method (see Appendix section). In Section "Information theory and complexity measures", the analytic expression obtained for the eigenfunction will applied to study the information entropy and complexity measures in Interstellar mediums, and finally the concluding remark in Section "Conclusion".

Eigen solution

To obtain the eigensolution for the electric screening potential of Eq. (1), we employ the Schrödinger equation in one dimension of the form [31],

$$\frac{d^2\psi(x)}{dx^2}+\frac{2m}{\hbar^2}\left[E-V(x)-\frac{l(l+1)\hbar^2}{2\,mx^2}\right]\psi(x)=0 \tag{3}$$

where m and $\hbar^2$ are the reduced mass and Planck constant, respectively. Substituting the potential into Eq. (3), we obtain

$$\frac{d^2\psi(x)}{dx^2}+\frac{2m}{\hbar^2}\left[E-\frac{1}{4\pi\epsilon_0}\frac{q_1q_2}{x}e^{-\alpha x}-\frac{l(l+1)\hbar^2}{2\mu x^2}\psi(x)\right]=0 \tag{4}$$

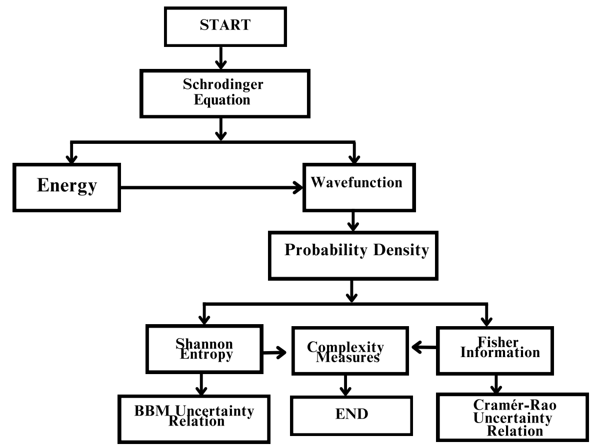

Fig. 1. Flow Chart. The study begins with obtaining an analytic solution of the energy wave function of the electrical screening potential using the Schrodinger equation. With the probability density, we extend our study to Shannon entropy, Fisher information and their complexity measures. The uncertainty relations are verified for Shannon entropy and Fisher information.

Eq. (4) cannot be solved exactly ($l \neq 0$), we use the Greene and Aldrich approximation [9,32] and the coordinate transformation, $y = e^{-2\alpha x}$, to obtain the hypergeometric function

$$\frac{d^2\psi(y)}{dy^2}+\frac{(1-y)}{y(1-y)}\frac{d\psi(y)}{dy}+\frac{1}{y^2(1-y)^2}\left[-\kappa z^2+Qz-\zeta\right]\psi(y)=0 \tag{5}$$

where

$$\left.\begin{aligned}\kappa &= \beta-\chi\\ Q &= 2\beta-\chi-L\\ \zeta &= \beta\end{aligned}\right\} \tag{6}$$

$\chi = \frac{Ae^2\mu}{\alpha\hbar^2}$, $\beta = -\frac{\mu E}{2\alpha^2\hbar^2}$, $E < 0$, and $L = l(l+1)$. To obtain the energy value and the wave function, we adopt the NUFA method (see Appendix). Hence, We compare Eq. (5) with (A.27)

$$\gamma_1=\gamma_2=\gamma_3=1, \xi_1=\kappa, \xi_2=Q, \xi_2=\zeta$$

The energy of electrical screening potential is

$$E_{nl} = -\frac{2\alpha^2\hbar^2}{m}\left[\frac{-\frac{Ame^2}{\alpha\hbar^2}+(n+l+1)^2}{2(n+l+1)}\right]^2 \tag{7}$$

where, $m = \hbar^2 = 1$, $A = \frac{1}{4\pi\varepsilon}$ and n is the quantum number. $\alpha = 1/D$, where D is The Debye length in the interstellar mediums ($D = 10^1$ m) [1]. The charges are $e^2 = q_1q_2 = (1.69\times10^{-19}\ \mathrm{C})^2$, and $\varepsilon = \varepsilon_r\varepsilon_0$. We take $\varepsilon_r = 1$ and ε_0 as the permittivity of free space, 8.85419×10^{-12} F/m. The energy equation shows that α influences the outcome significance such that as α increases, the energy becomes more negative. However, the impact ofα is mitigated by the values of n and l. Also, we obtain the corresponding wave function in terms of the Gauss hypergeometric function,

$$\psi(y) = N_n y^\lambda(1-y)^\upsilon {}_2F_1(-n, n+2(\lambda+\upsilon); 1+2\lambda; y) \tag{8}$$

where, $y = e^{-2\alpha x}$, $\lambda = \sqrt{\beta}$, $\upsilon = l+1$. N_n is the normalization constant. The hypergeometric function of Eq. (8) can be expressed in terms of the Jacobi Polynomial [33]

$${}_2F_1(-n, n+2(\lambda+\upsilon); 1+2\lambda; y) = \frac{\Gamma(2\lambda)\Gamma(n)}{\Gamma(n+2\lambda)}P_n^{2\lambda,2\upsilon}(1-2y) \tag{9}$$

We rewrite Eq. (8) in terms of Jacobi polynomial as

$$\psi(y) = N_n\frac{\Gamma(2\lambda)\Gamma(n)}{\Gamma(n+2\lambda)}y^\lambda(1-y)^\upsilon P_n^{2\lambda,2\upsilon}(1-2y) \tag{10}$$

where $P_n^{2\lambda,2\upsilon}(1-2y)$ is the Jacobi of the nth polynomial. To obtain the normalization constant, the wavefunction is written as

$$\psi(y) = N_n y^{\lambda}(1-y)^{\upsilon} P_n^{2\lambda,2\upsilon}(1-2y), \qquad y = e^{-2\alpha x} \tag{11}$$

The normalization is given by

$$N_n = \left[\int_0^{\infty} |\psi(x)|^2 dx\right]^{-1/2} = \left[\frac{1}{2\alpha}\int_0^1 |\psi(y)|^2 \frac{dy}{y}\right]^{-1/2} \tag{12}$$

We adopt MATHEMATICA 12.0 Software to obtain the analytic expression of the normalized wavefunction for the ground state and first excited state in the position space. Due to complexity, the higher states ($n = 2-4$) will be solved numerically. Therefore,

$$\psi_0(x) = \sqrt{\frac{2\alpha\Gamma(2\lambda+2\upsilon+1)}{\Gamma(2\lambda)\Gamma(2\upsilon+1)}}e^{-2\alpha\lambda}(1-e^{-2\alpha x})^{\upsilon} \tag{13}$$

$$\psi_1(x) = N_1\left(e^{-2\alpha r}\right)^{\lambda+1}\left(1-e^{-2\alpha r}\right)^{\upsilon}\times \left[\frac{\left(-2\lambda+2\lambda e^{2\alpha r}+e^{2\alpha r}-2\upsilon-1\right)}{2\lambda+1}\right] \tag{14}$$

where,

$$N_1 = \sqrt{\frac{2\lambda\alpha(2\lambda+1)^2\Gamma(2\lambda+2\upsilon+3)}{(\upsilon+1)(2\lambda+2\upsilon+1)\Gamma(2+2\lambda)\Gamma(2\upsilon+1)}} \tag{15}$$

The probability density in the momentum space is obtained using the Fourier transform in one dimension defined as [33],

$$\phi(p) = \frac{1}{\sqrt{2\pi}}\int \psi(x)e^{-ipx}dx \tag{16}$$

We obtained the expression for the normalized wavefunction of momentum space for the ground state and excited states as,

$$\phi_0(p) = \frac{N_0}{\sqrt{2\pi}}\frac{\Gamma(\upsilon+1)\Gamma\left(\frac{ip}{2\alpha}+\lambda\right)}{2\alpha\Gamma\left(1+\frac{ip}{2\alpha}+\lambda+\upsilon\right)} \tag{17}$$

$$\phi_1(p) = \frac{N_1}{\sqrt{2\pi}}\Gamma(-ip\upsilon+\alpha(1+\upsilon+2\lambda))\times \frac{\Gamma(1+\upsilon)\Gamma\left(\frac{ip}{2\alpha}+\lambda\right)}{2\alpha^2(2\lambda+1)\Gamma\left(\frac{ip}{2\alpha}+\lambda+\upsilon+2\right)} \tag{18}$$

The probability density plots in Fig. 2 for interstellar mediums show the localization increases as it moves away from the ground state. On the other hand, localization decreases as you as n increases. This behaviour conforms to the uncertainty principle. The following section, explores Shannon entropy, Fisher information and complexity measure. Probability density is an essential component of these statistical measures.

Information theory and complexity measures

Shannon's entropy measurements are just probabilistic measurements that help us more precisely analyse the possible location of the quantum particle. Shannon's theory emerged as measuring the loss of information transmitted between a transmitting source and a receiving source [12]. Because this theory works with a probability density, it was easily applied to quantum theories by measuring the loss of information about the particle's location, thus becoming a powerful tool in the study of predictions of possible experimental detections of quantum particles. This motivates us to calculate Shannon entropy measures for our model.

Shannon entropy is a global variable concerned with the degree of randomness (or smoothness) and uncertainty within a localized space [9]. The uncertainty relation unifies the position and momentum space of the Shannon entropy, proving to be a better version of the Heinsberg relation as it accounts for high order in this domain [14]. The Shannon entropy has a logarithmic factor, and it is defined as

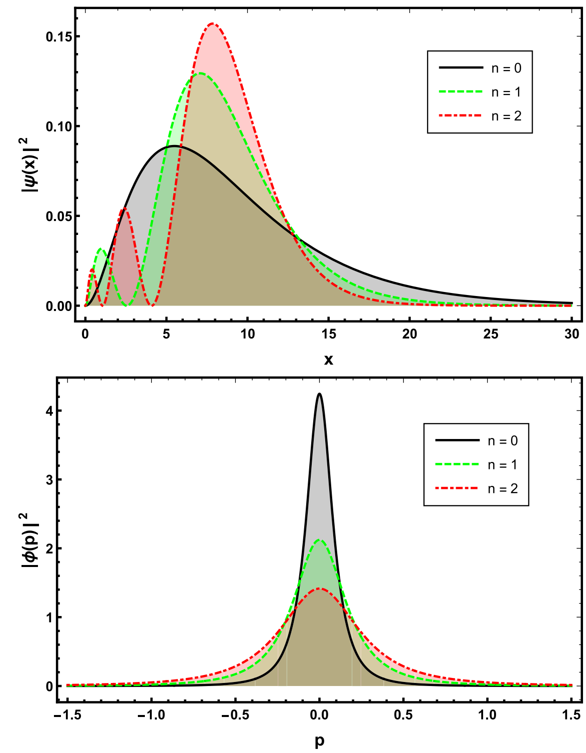

Fig. 2. (a) and (b) are density plots of the position and momentum space respectively for low-lying states at $l = 0$ for interstellar mediums ($D = 10^1$).

$$S_x = -\int \rho(x)\log[\rho(x)]dx \tag{19}$$

$$S_p = -\int \phi(p)\log[\phi(p)]dp \tag{20}$$

where S_x and S_p are the Shannon in position and momentum space in one dimension, respectively. $\rho(x) = |\psi(x)|^2$ is the probability density in position space and $\phi(p) = |\phi(p)|^2$ is the probability density in momentum space. The BBM uncertainty relations for the Shannon entropy [34,35] given by,

$$S_x + S_p \geq (1+\ln\pi) \geq 2.1477 \tag{21}$$

Due to the complexity of the integrals involved in Shannon entropy, we obtained numerical results in position, S_x and momentum space, S_p in Table 1 (left). for n and l values. Our result showed that Shannon entropy values decrease when n and l are increased. Here, the particle becomes more localized and decreases uncertainty in predicting the particle location. Conversely, in the momentum space, S_p, Shannon entropic values increase for n and l. Furthermore, the entropic relation of the position and momentum space validates the BBM relation in Eq. (21).

On the other hand, Fisher information is a local variable and considers the intrinsic properties of the probability distribution of the system. Fisher information can also be seen as fluctuation parameters because of the kinetic energy term it possesses [36]. Fisher information is a probability density functional defined as

$$I_x = \int \frac{[\rho'(x)]^2}{\rho(x)}dx = 4\int |\phi'(x)|^2 dr = 4\langle p^2\rangle \tag{22}$$

$$I_p = \int \frac{[\phi'(p)]^2}{\phi(p)}dp = 4\int |\psi'(p)|^2 dp = 4\langle x^2\rangle \tag{23}$$

Table 1
Numerical values of Shannon Entropy and Fisher information calculated for the first four principal quantum numbers, $n = 0, 1, 2, 3, 4$.

n	l	S_x	S_p	S_{x+p}	I_x	I_p	$I_x I_p$
0	0	3.01083	−0.291246	2.71958	0.12	472.222	56.677
1	0	2.64114	0.0553264	2.69647	0.48	350.056	168.027
	1	2.45778	0.208965	2.66675	0.60	288.708	173.225
2	0	2.475	0.0890615	2.56406	1.08	327.239	353.418
	1	2.36744	0.237279	2.60472	1.28	297.891	381.300
	2	2.28343	0.332934	2.61636	1.56	274.129	427.641
3	0	2.37443	0.40189	2.77632	1.92	319.233	612.927
	1	2.3012	0.501907	2.80311	1.22	301.962	664.315
	2	2.24069	0.570622	2.81131	2.59	285.026	738.217
	3	2.18809	0.620278	2.80837	3.00	270.115	810.33
4	0	2.30473	0.513451	2.81818	3.00	315.523	946.57
	1	2.25048	0.597787	3.41597	3.36	304.126	1021.86
	2	2.20408	0.659946	3.47813	3.86	291.482	1126.28
	3	2.16272	0.706986	3.52517	4.39	279.428	1226.29
	4	2.12506	0.743718	3.5619	4.92	268.463	1320.84

Table 2
Numerical values for complexity measures in the position and momentum regimes for four different values of principle quantum number n.

n	l	$b = 1$		$b = 2/3$	
		C_x	C_p	C_x	C_p
0	0	2.43651	352.907	0.89311	388.886
1	0	6.73398	369.969	2.79208	363.208
	1	7.00734	355.804	3.08854	331.864
2	0	12.8322	357.72	5.62352	347.257
	1	13.6576	377.665	6.20373	348.945
	2	15.3041	382.4252	7.14901	342.255
3	0	20.6303	477.14	9.34911	417.317
	1	21.9696	498.801	10.2021	421.957
	2	24.3643	504.316	11.5447	416.962
	3	26.7544	502.263	12.9014	408.448
4	0	30.0644	527.254	13.9447	444.315
	1	31.8942	552.928	15.0633	453.033
	2	35.0153	563.926	16.7952	452.569
	3	38.1575	566.645	18.5564	447.676
	4	41.1971	564.777	20.2877	440.771

$\phi'(x)$ and $\psi'(p)$ are the first derivative function of$x$ and p, respectively, and I_x I_p are Fisher information in position and momentum space in one dimension, respectively. The Cramér–Rao uncertainty relation for the Fisher information [37]

$$I_x I_p \geq 36 \tag{24}$$

The numerical obtained for Fisher information in Table 1 (right) showed an increasing fluctuation of the particle and consequently the probability density becomes more localized, and there is higher accuracy in predicting the localization of the particle in position space for n and l. For the momentum space, for increasing value of n and l showed a decreasing trend. The accuracy in predicting the particle localization is low, and uncertainty is high. Furthermore, we have shown that the Cramer-Rao uncertainty relation for Fisher Information of Eqs. (24) is satisfied.

Complexity measures are statistical tools that combine local and global variables. For any system, complex measures lie between extremes of order and disorder. It explains the correlation and structure of quantum systems. The general form of complexity takes the form [38] $C_{A,B} = Ae^{bB}$, where A and B represent the order and disorder, respectively. For Fisher–Shannon complexity, it is defined as,

$$C_{IS} = I e^{bS}, \tag{25}$$

where I, is the Fisher information and it represent order, and b is the scaling factor. Invariance under scaling has been satisfied for complexity measures. we considered the scaling factor, $b = 1, 2/3$ for position and momentum spaces, respectively. [14,38,39], and as a result of its scaling invariant property, $b = 1$ is equivalent to C_{IS} at $b = 2/3$. The numerical analysis was also carried out for complexity measures as reported in Table 2. Our result showed that an increasing value of n and l escalates the complexity values for both scaling parameters. Hence, shows an indication of disorder in the system.

To gain more insight into the study, we extend the Debye–Hückel length, D, to other domains such as the Magnetosphere ($D = 10^2$) and Intergalactic Mediums ($D = 10^5$) in the ground state in position space. As D increases, the screening parameter gets smaller, making the electrostatic interaction stronger for Shannon entropy where probability density becomes more localized, and increases measurement sensitivity for Fisher Information. Increasing the Debye–Huckel length at the ground state is presented in Figs. 3–6. Figs. 3 and 4 represent the Shannon entropy in the ground state for different D regimes. As the value of D increases, the Shannon entropic values in position space Fig. 3 decrease and the peak distance increases while it decreases for the momentum space in Fig. 4. For the Fisher information in position space in Fig. 5 and momentum space in Fig. 6. As the D regime increases, $I(x)$ values get smaller and increases for $I(p)$.

Conclusion

Using the Shannon entropy, Fisher information, and Complexity measures, we explored the probability density properties for interstellar mediums for the various values of n for the screening potential. Using the Schrodinger equation, we obtained the energy equation and wavefunction using the NUFA method. We carried out a graphical study on the probability density distribution for the potential for the increasing value of n in position and momentum space. Numerical analysis was carried out on Shannon entropy and Fisher information in position and momentum space and their uncertainty in predicting localization as the value of n increases. For more insight, we extended the Debye–Huckel length to the Magnetosphere and intergalactic mediums for the ground state. Numerical analysis for complexity measures shows a disorder in the system due to an increasing value of n in the position space.

CRediT authorship contribution statement

Precious O. Amadi: Writing – original draft, Software, Investigation. **Suryadi Suryadi:** Writing – review & editing, Supervision, Formal analysis. **Norshamsuri Ali:** Writing – original draft, Validation, Supervision, Funding acquisition. **Syed Alwee Aljunid:** Writing – review & editing, Supervision. **Rosdisham Endut:** Writing – review & editing, Validation, Funding acquisition. **Mohd Aminudin Jamlos:** Validation, Funding acquisition. **Akpan N. Ikot:** Writing – review & editing, Supervision, Conceptualization.

Declaration of competing interest

We wish to confirm that there are no known conflicts of interest associated with this publication.

Data availability

No data was used for the research described in the article.

Acknowledgements

The authors would also like to acknowledge the support from the Long Term Research Grant Project under a grant number of LRGS/1/2020/UM/01/5/4 from the Ministry of Higher Education Malaysia (MOHE). This work was partly supported by the DIKTI (Directorate General of Higher Education) Indonesia Grant (No.: 179/ES/PG.02.00PL/2023, 1402/LL3/AL.04/2023, 149/VRRTT/VI/2023).

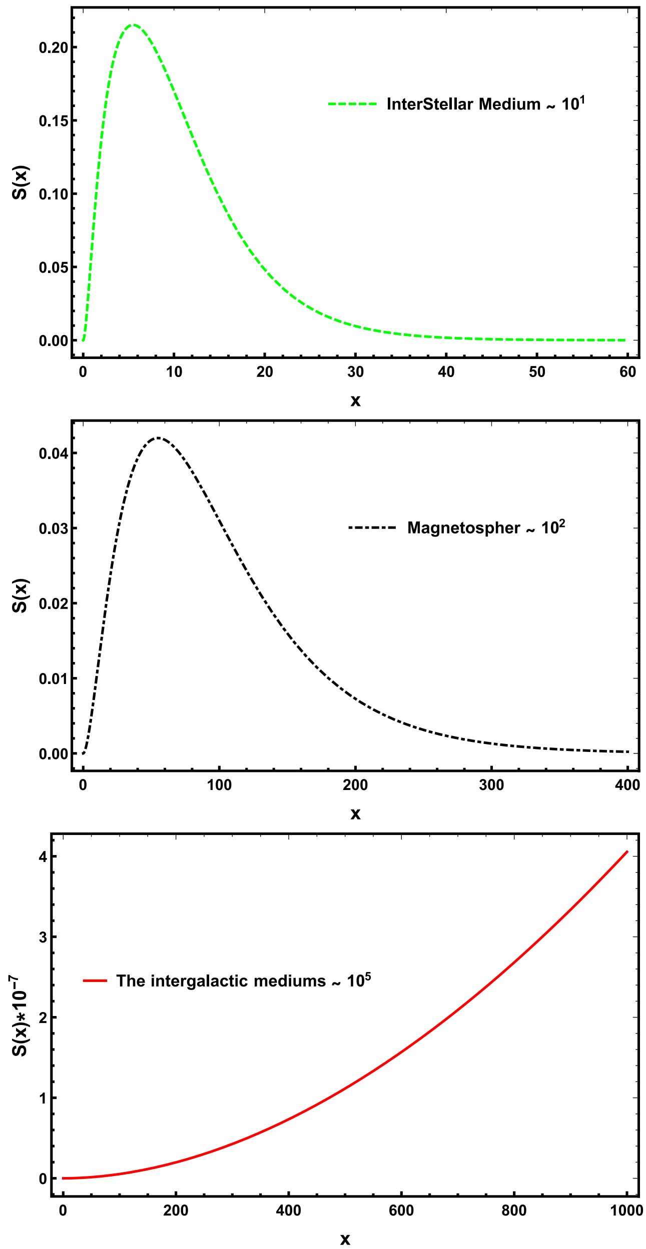

Fig. 3. Shannon Entropy in the Ground state in position space for different Debye-Hückel lengths, Interstellar Mediums, 10^1, Magnetosphere, 10^2, and The intergalactic mediums, 10^5 [1].

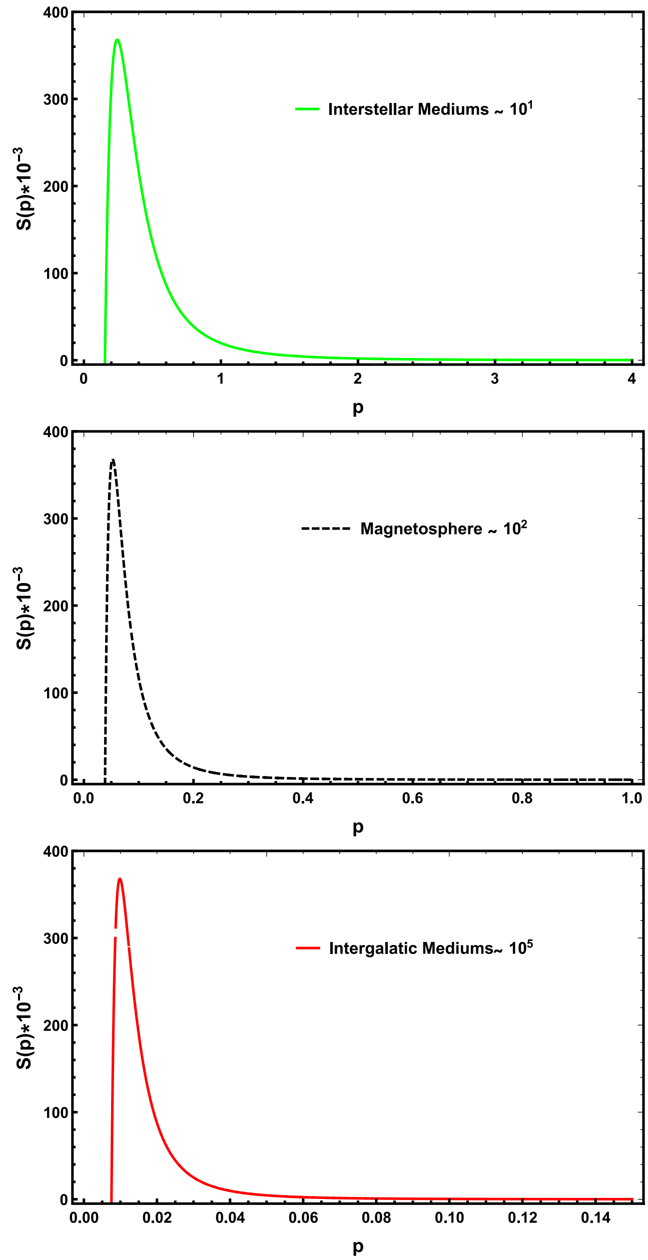

Fig. 4. Shannon Entropy in the Ground state in momentum space for different Debye–Hückel lengths, Interstellar Mediums, 10^1, Magnetosphere, 10^2, and The intergalactic mediums, 10^5 [1].

Appendix

The Nikiforov–Uvarov-Functional Analysis (NUFA) method [40] and the references therein were developed based on the ideas of the NU method, parametric NU method, and the functional analysis to solve second-order differential equations of the hypergeometric type of the form

$$\psi_n''(s) + \frac{\tilde{\tau}(s)}{\sigma(s)}\psi_n'(s) + \frac{\tilde{\sigma}(s)}{\sigma^2(s)}\psi_n(s) = 0 \tag{A.26}$$

where $\sigma(s)$ and $\tilde{\sigma}(s)$ are polynomial, at most of second degree, and $\tilde{\tau}(s)$ is first-degree polynomial. The parametric form of the NU method is the form

$$\psi_n''(s) + \frac{\gamma_1 - \gamma_2 s}{s(1-\gamma_3 s)}\psi' + \frac{1}{s^2(1-\gamma_3 s)^2}[-\xi_1 s^2 + \xi_2 s - \xi_3]\psi_n(s) = 0 \tag{A.27}$$

where, γ_i and $\xi_i (i = 1, 2, 3)$ are all parameters. It can be observed in Eq. (A.27) two singularities at $s \to 0$ and $s \to 1$, the wave function takes the form,

$$\psi(s) = s^{\lambda}(1-s)^{\upsilon} f(s) \tag{A.28}$$

Substituting Eq. (A.28) into Eq. (A.27) we have,

$$s(1-\gamma_1 s)f''(s) + [\gamma_1 + 2\lambda(2\lambda\gamma_3 + 2\upsilon\gamma_3 + \gamma_2)s]f'(s) - \alpha_3\left(\lambda + \upsilon + \frac{\gamma_2}{\gamma_3} - 1 + \sqrt{\left(\frac{\gamma_2}{\gamma_3} - 1\right)^2 + \frac{\xi_1}{\gamma_3}}\right)\times \left(\lambda + \upsilon + \frac{\gamma_2}{\gamma_3^2} - 1 + \sqrt{\left(\frac{\gamma_2}{\gamma_3} - 1\right)^2 + \frac{\xi_1}{\gamma_3^2}}\right) +$$

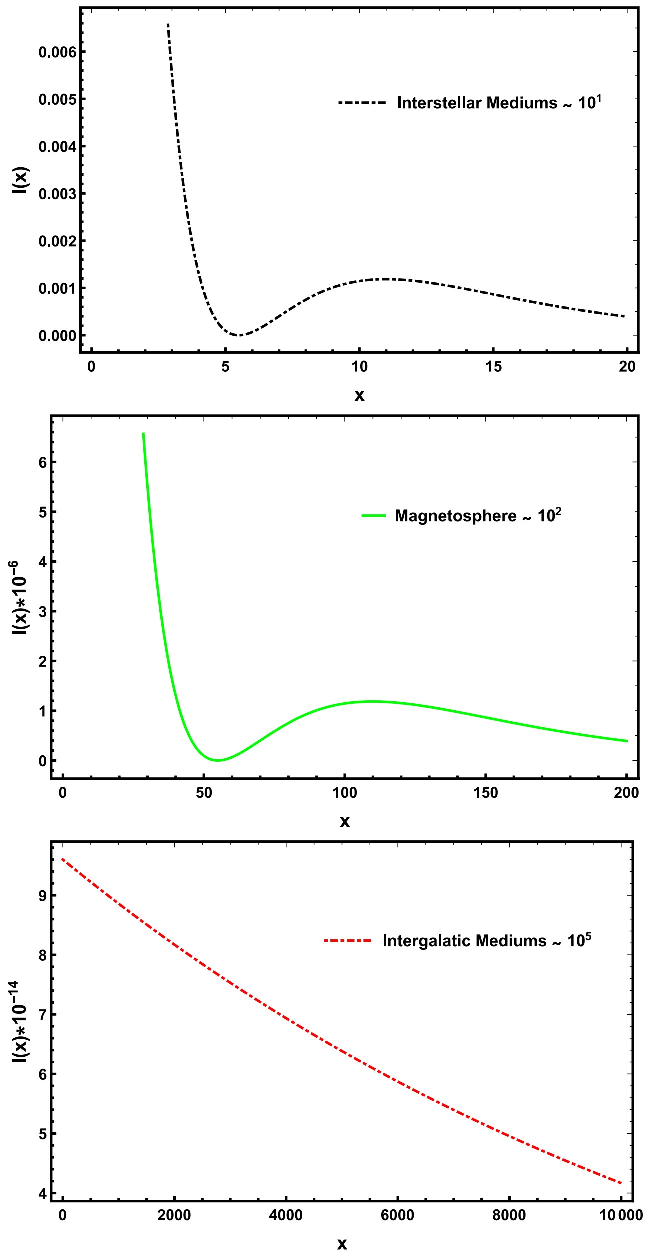

Fig. 5. Fisher Information in the ground state in position space for different Debye-Hückel lengths, Interstellar Mediums, 10^1, Magnetosphere, 10^2, and The intergalactic mediums, 10^5 [1].

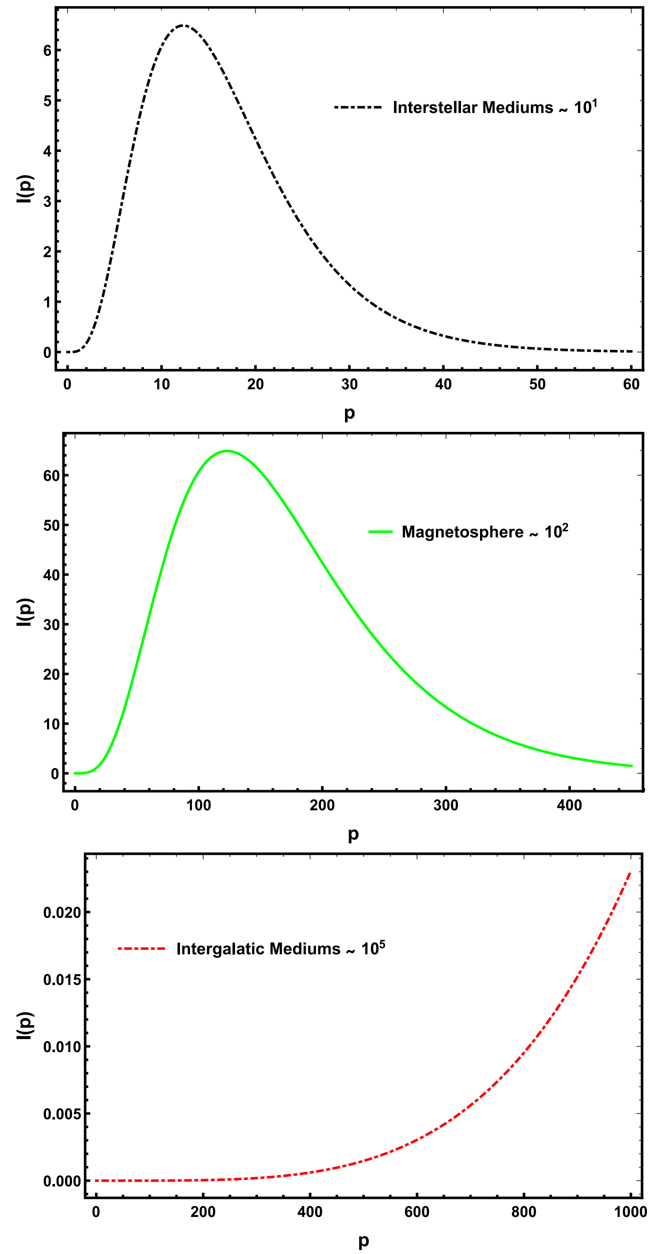

Fig. 6. Fisher Information in the ground state in momentum space for different Debye-Hückel lengths, Interstellar Mediums, 10^1, Magnetosphere, 10^2, and The intergalactic mediums, 10^5 [1].

$$\left[\frac{\lambda(\lambda-1)+\gamma_1\lambda-\xi_3}{s}+\frac{\gamma_2 v-\gamma_1\gamma_3 v+v(v+1)\gamma_3-\frac{\xi_1}{\gamma_3}+\xi_2-\xi_3\gamma_3}{1-\gamma_3 s}\right]f(s)=0 \tag{A.29}$$

Solving Eqs. (23) and (25) completely give,

$$\lambda=\frac{(1-\gamma_1)\pm\sqrt{(1-\gamma_1)^2+4\xi}}{2}$$
$$v=\gamma_3(1+\gamma_1)-\gamma_2\pm\frac{\sqrt{(\gamma_3(1+\gamma_1)\gamma_2)^2+4\left(\frac{\xi_1}{\gamma_3}+\gamma_3\xi_3-\xi_2\right)}}{2} \tag{A.30}$$

The hypergeometric equation type of Eq. (25) takes the form,

$$x(1-x)f''(x)+[c+(a+b+1)x]f'(x)-abf(x)=0 \tag{A.31}$$

where a, b, c are given by

$$a=\sqrt{\gamma_3}\left[\lambda+v+\frac{\gamma_2}{\gamma_3}-1+\sqrt{\left(\frac{\gamma_2}{\gamma_3}-1\right)^2+\frac{\xi_1}{\gamma_3}}\right] \tag{A.32}$$

$$b=\sqrt{\gamma_3\left[\lambda+v+\frac{\gamma_2}{\gamma_3}-1-\sqrt{\left(\frac{\gamma_2}{\gamma_3}-1\right)^2+\frac{\xi_1}{\gamma_3}}\right]} \tag{A.33}$$

$$c=\gamma_1+2\lambda \tag{A.34}$$

The energy equation is obtained as follows:

$$\lambda^2 + 2\lambda\left[\upsilon + \frac{\gamma_2}{\gamma_3} - 1 + \frac{n}{\sqrt{\gamma_3}}\right] + \left[\upsilon + \frac{\gamma_2}{\gamma_3} - 1 + \frac{n}{\sqrt{\gamma_3}}\right]^2 - \left[\frac{\gamma_2}{\gamma_3} - 1\right] - \frac{\xi^3}{\gamma_3^2} = 0 \quad (A.35)$$

and its wave equation,

$$\psi(s) = N s^{\lambda}(1 - \gamma_3 s)^{\upsilon}{}_2F_1(a, b, c; s) \quad (A.36)$$

References

[1] Marwan Al-Reei. Chaos Solitons Fractals 2021;150:111209.
[2] Singh AK, Dawra D, Dimri M, Jha AK, Pandey R, Mohan M. Phys Letts A 2020;384(12):126369.
[3] Stolz H, Semkat D, Schwartz R, Heckötter J, Aßmann M. 105 (7).
[4] Zeng J, Li Y, J. Yuan. J Quant Spectrosc Radiat Transfer 2021;272:107777.
[5] Soylu A. Phys Plasmas 2012;19:072701. http://dx.doi.org/10.1063/1.4736947.
[6] Koyuncu F, Soylu A. Chinese Phys C 2018;42(5):054106.
[7] Jiao LG, Zan LR, Zhu L, Ma J, Ho YK. Comp phys comm. 2019;244:217–27.
[8] Paul S, Ho YK. Phys Plasmas 2005;16:063302.
[9] Isonguyo CN, Oyewumi KJ, Oyun OS. Int J Quantum Chem 2008;118:025620.
[10] Paul S, Ho YK. Phys Plasmas 2010;17:082704.
[11] Gargaud M, Amils R, editors. Encyclopedia of astrobiology. vol. 1, Springer Science & Business Media; 2011.
[12] Shannon CE. Bell Syst Tech J 1948;27(379).
[13] Fisher RA. Proc Camb Phil Soc 1925;22(700).
[14] Majumdar S, Mukherjee N, Roy AK. Chem Phys Lett 2019;716:257–64.
[15] Abdel-Hady A, Nasser I. Appl Math Inf Sci 2018;12(4).
[16] Nagy A. Int J Quantum Chem 2015;115(1392).
[17] Chatterjee S, Sekh GA. Report Math Phys 2020;2:85, Rampho, and H. Y. Abdullah Int J Quant Chem 120, e26246.
[18] Pooja Kumar R, Kumar G, Kumar R, Kumar A. Int J Quantum Chem 2016;116(19).
[19] Salazar SJ, Laguna HG, Prasad V, Sagar RP. Int J Quant Chem 2020;120(11).
[20] Amadi PO, Ikot AN, Ngiangia AT, Okorie US, Rampho GJ. Int J Quantum Chem 2020;120(14).
[21] Amadi PO, Ikot AN, Rampho GJ, Okorie US, Abdullah HY, Lutfuoglu BC. Rev Mex Fis 2020;66(6).
[22] Ikot AN, Rampho GJ, Amadi PO, Okorie US, Sithole MJ, Lekala ML. Int J Quantum Chem 2020;120(24).
[23] Roy AK. Modern Phys Lett A 2014;29:1450104.
[24] Ghosal A, Mukherjee N, Roy AK. Ann Phys (Berlin) 2016;528(796).
[25] Yaha WA, Oyewumi KJ, Sen KD. Int J Quantum Chem 2015;115(1543).
[26] Valencia-Torres R, Guo-Hua S, Dong SH. Phys Scr 2015;90:035205.
[27] Dong S, Sun GH, Dong SH, Draayer JP. Phys Lett A 2014;378(124).
[28] Edet CO, Ikot AN. Eur Phys J 2021;4(136).
[29] Mukherjee N, Roy AK. Int J Quantum Chem 2018;e25596.
[30] Udoh ME, Amadi PO, Okorie US, Antia AD, Obagboye LF, Horchani R, et al. Pramana - J Phys 2022;96(222).
[31] Osobonye GT, Okorie US, Amadi PO, Ikot AN. Can J Phys 2021;99(7).
[32] Greene RL, Aldrich C. Phys Rev A 1976;14(2363).
[33] Abramowitz M, Stegun IA, Romer RH. Handbook of mathematical functions with formulas, graphs, and mathematical tables. 1988, http://dx.doi.org/10.1119/1.15378.
[34] Bialynicki-Birula I, Mycielski J. Comm Math Phys 1975;44(129).
[35] Beckner W. Ann Math 1975;102(159).
[36] Sears SB, Parr RG, Dinur U. Israel J Chem 1980;19(165).
[37] Romera E, Sanchez-Moreno P, Dehesa JS. Chem Phys Lett 2005;414(468).
[38] Majumdar S, Mukherjee N, Roy AK. Chem Phys Lett 2017;687(322).
[39] Mukherjee N, Roy AK. J Math Chem 2019;57(7).
[40] Ikot AN, Okorie US, Amadi PO, Edet CO, Rampho GJ, Sever R. Few-Body Syst 2021;62:1–16.